Anatomy of an extinct magmatic system along a divergent plate boundary: Alftafjordur, Iceland

S. Urbani, D. Trippanera, M. Porreca, C. Kissel, V. Acocella

AGU PUBLICATIONS

Geophysical Research Letters

RESEARCH LETTER
10.1002/2015GL065087

Key Points:
- Diking is the key mechanism for crustal spreading
- Prevalent subvertical magma propagation, along divergent plate boundaries, at ~1.5 km depth
- Crustal spreading in eastern Iceland at 10–12 Ma was slower than present

Supporting Information:
- Supporting Information S1
- Figure S1
- Figure S2
- Figure S3
- Figure S4
- Figure S5
- Table S1

Correspondence to:
S. Urbani,
stefano.urbani@uniroma3.it

Citation:
Urbani, S., D. Trippanera, M. Porreca, C. Kissel, and V. Acocella (2015), Anatomy of an extinct magmatic system along a divergent plate boundary: Alftafjordur, Iceland, *Geophys. Res. Lett.*, *42*, 6306–6313, doi:10.1002/2015GL065087.

Received 26 JUN 2015
Accepted 21 JUL 2015
Accepted article online 24 JUL 2015
Published online 13 AUG 2015

Anatomy of an extinct magmatic system along a divergent plate boundary: Alftafjordur, Iceland

S. Urbani[1], D. Trippanera[1], M. Porreca[2,3], C. Kissel[4], and V. Acocella[1]

[1]Dipartimento di Scienze, Università Roma Tre, Rome, Italy, [2]Dipartimento di Fisica e Geologia, Università di Perugia, Perugia, Italy, [3]Istituto Nazionale di Geofisica e Vulcanologia, L'Aquila, Italy, [4]Laboratoire des Sciences du Climat et de l'Environnement, CEA-CNRS-UVSQ, Gif-sur-Yvette, France

Abstract Recent rifting episodes highlight the role of magmatic systems with propagating dikes on crustal spreading. However, our knowledge of magmatic systems is usually limited to surface observations and geophysical data. Eastern Iceland allows direct access to extinct and eroded deeper magmatic systems. Here we collected field structural and AMS (anisotropy of magnetic susceptibility) data on 187 and 19 dikes, respectively, in the 10–12 Ma old Alftafjordur magmatic system. At a paleodepth of ~1.5 km, the extension due to diking is at least 1–2 orders of magnitude larger than that induced by regional tectonics, confirming magmatism as the key mechanism for crustal spreading. This magma-induced extension, inferred from the aspect ratio of the magmatic system, was of ~8 mm/yr, lower than the present one. AMS data suggest that most of dikes have geometrically normal fabric, at least at the margins, consistent with prevalent subvertical magma flow and propagation.

1. Introduction

Recent rifting episodes in Iceland and Afar highlight the importance of magmatic systems [*Gudmundsson et al.*, 2014] with lateral propagation of dikes along the rift axis in achieving crustal spreading [*Acocella*, 2014; *Sigmundsson et al.*, 2015]. Magmatic systems are crustal portions, tens of kilometers long and few kilometers wide, where fracturing and faulting are associated with fissural monogenic mafic eruptions and a central, felsic, or mafic volcano [*Gudmundsson*, 1995; *Ebinger and Casey*, 2001]. Our knowledge of magmatic systems and related rifting processes is usually restricted to the surface, where geological and geodetic data are collected. In some cases, geophysical information is available, as for active seismicity during rifting events [*Ebinger et al.*, 2010; *Sigmundsson et al.*, 2015] or seismic refraction profiles and magnetotelluric data [*Brandsdottir et al.*, 1997; *Desissa et al.*, 2013]. However, in these cases the resolution on the structure of the magmatic systems is much more limited than that available at the surface. Crucial information on the magma storage and propagation, and its relationship with regional tectonics, may be obtained in the deeper portion of the magmatic systems. Eastern and western Iceland provide the rare opportunity to study several extinct and eroded magmatic systems at a paleodepth of 1–2 km. Here several studies show the occurrence of dike swarms, with iso-oriented dikes usually decreasing in frequency toward the surface, associated with shallow magma chambers [*Walker,* 1958, 1960, 1963; *Gudmundsson*, 1983, 1995; *Helgason and Zentilli,* 1985; *Paquet et al.*, 2007].

This study is aimed at better (1) defining the structural features of the deeper part of extinct magmatic systems along divergent plate boundaries and (2) unraveling the tectono-magmatic relationships responsible for the processes operating within magmatic systems. To these aims, we collected field structural and AMS (anisotropy of magnetic susceptibility) data on dikes in the 10–12 Ma old Alftafjordur magmatic system, eastern Iceland. In eastern Iceland there are five inactive volcanic systems exposed at a paleodepth of ~1.5 km (Figure 1) [*Walker,* 1974; *Paquet et al.,* 2007]. These consist of a thousand subvertical dikes, with mean thickness of 3–4 m [*Gudmundsson,* 1983; *Helgason and Zentilli,* 1985; *Paquet et al.*, 2007]. Estimated magmatic extensions range from 1% to 12%, decreasing with altitude [*Walker,* 1958, 1960; *Gudmundsson,* 1995; *Paquet et al.,* 2007]. The Alftafjordur magmatic system is the extinct portion of a 10–12 Ma old rift consisting of a central volcano (to the south) and a 30–40 km long NNE-SSW trending dike swarm (Figure 1) [*Moorbath et al.,* 1968; *Walker,* 1974; *Gudmundsson,* 1995; *Paquet et al.,* 2007].

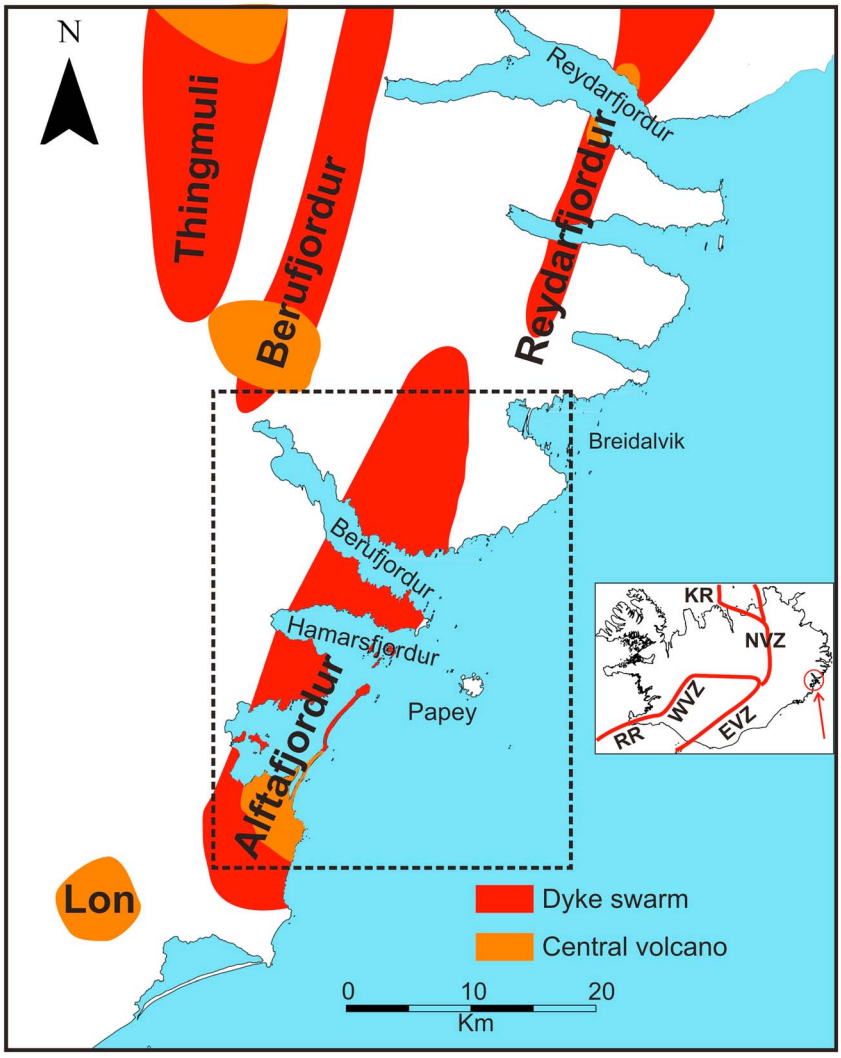

Figure 1. Extinct magmatic systems in Eastern Iceland (from *Paquet et al.* [2007]). The black rectangle indicates the area of Figure 2. Inset indicates the active rift zones in Iceland. The red circle and arrow locate the studied area.

2. Methods

2.1. Structural Field Analysis

Structural field data focus on the geometry and kinematics of extension fractures, faults, and dikes. For each extension fracture and fault we measured attitude, displacement (opening or shear), and frequency; whereas for dikes we measured the attitude, thickness, flow direction of magma within (using striations, elongated vesicles or minerals), and frequency. Our measurements focused on four sections of variable length (from 1.5 to 12 km), orthogonal to the swarm trend (1 to 4 in Figure 2a). Here we also calculated the extension due to diking (sum of the thicknesses of 165 dikes) and that due to faulting (sum of the horizontal throws). We focused our observations at elevation slightly above the sea level, to avoid any dike frequency variation due to elevation [*Walker,* 1974; *Gudmundsson,* 1983]. We calculated the across-strike variations in dike frequency along the entire system, including previous results [*Gudmundsson,* 1995; *Paquet et al.,* 2007] where needed.

2.2. AMS: Methods and Sampling

AMS data are acquired to infer the magmatic flow direction within dikes. The method allows defining the preferred alignment of the magnetic grains in the rock, which follow magmatic flow during dike emplacement. The AMS tensor is geometrically represented by an ellipsoid, with three principal

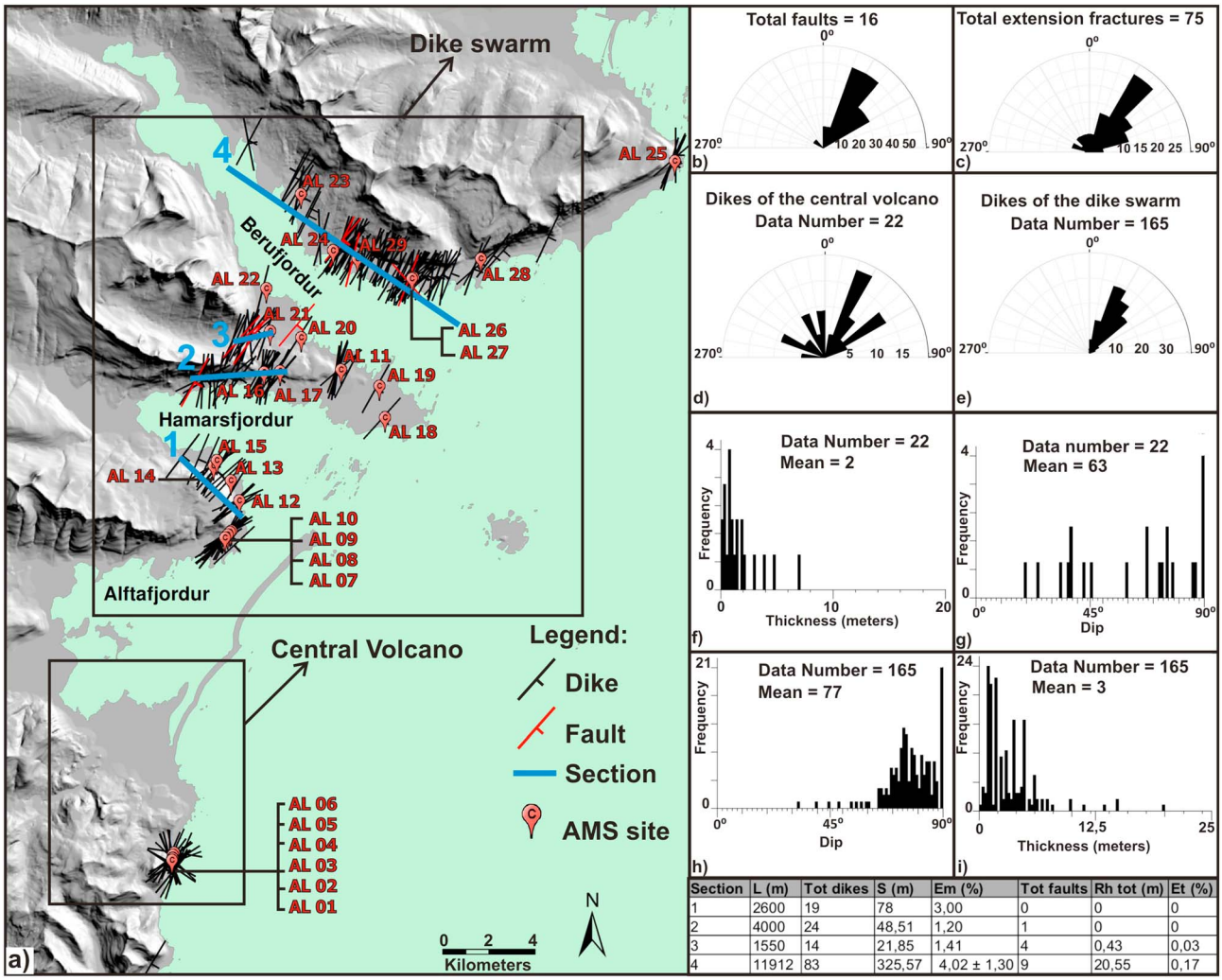

Section	L (m)	Tot dikes	S (m)	Em (%)	Tot faults	Rh tot (m)	Et (%)
1	2600	19	78	3,00	0	0	0
2	4000	24	48,51	1,20	1	0	0
3	1550	14	21,85	1,41	4	0,43	0,03
4	11912	83	325,57	4,02 ± 1,30	9	20,55	0,17

Figure 2. (a) DEM of the studied area showing the location and attitude of dikes and faults. The location of the sections and AMS sampling sites are also shown. The table at the bottom right shows the comparison between magmatic and tectonic extension for the four cross sections (see text for details). *L* = length of the section; *S* = total thickness of dikes; Rh = horizontal fault throw; Em = magmatic extension; Et = tectonic extension. Rose diagram of directions of (b) faults and (c) extension fractures of the volcanic system. Rose diagrams of directions, frequency histograms of the dip, and thickness of the dikes proximal to the central volcano (d, f, and g) and of the dikes belonging to the dike swarm (e, h, and i).

axes $K_{max} \geq K_{int} \geq K_{min}$. The magnetic fabric is usually related to the hydrodynamic forces of magma flow, and the magnetic lineation is usually consistent with other flow indicators, as vesicles or growth lineations, whereas magnetic foliation is parallel to the magmatic foliation [*Rochette et al.,* 1999; *Cañón-Tapia,* 2004].

Several AMS studies were conducted in eastern Iceland with contrasting interpretation on the magma flow directions, ranging from subvertical [*Craddock et al.*, 2008; *Kissel et al.*, 2010] to lateral [*Eriksson et al.*, 2011, 2015]. Here we present a synthesis of the low-field AMS results from 23 sites sampled in 19 dikes to try to define the magma flow propagation of the Alftafjordur dike swarm. We sampled each dike margin with more detail, measuring the main magnetic parameters (Figure S1 in the supporting information) and the orientations of the principal magnetic axes of the AMS ellipsoid. The orientation of magnetic foliations and lineations were used to infer magmatic flow directions. The AMS data were compared to orientations of minerals from thin section analysis and of field kinematic indicators. In particular, we performed image analysis of 14 oriented thin sections in four dikes, to compare the magnetic and mineral fabric, mainly in case of any anomalous (i.e., geometrically inverse fabric) orientation of the principal magnetic axes. Preferred orientations of phenocrysts (i.e., plagioclase) and opaque

minerals (i.e., Fe-Ti oxides) were analyzed using INTERCEPT software (see *Launeau et al.* [2010] for details on the method).

3. Results

3.1. General Features of the Magmatic System

The ~1 km thick Alftafjordur basaltic lava flow sequence shows a uniform strike at N250°, dipping between 5 and 10°. We recognized 187 dikes in the lava pile, 22 of which belong to the central volcano (as described by *Blake* [1969, 1970]) and 165 to the dike swarm (Figure 2b). The main strike of the dikes is NNE-SSW (72% of data set), with minor directions ranging from N331° to N20° (20% of data set) and from N51° to N70° (8% of the data set). Most dikes are steeply dipping or subvertical, with mean dip of 76°. Their mean thickness is 3.2 m, focusing in the 0.1–10 m range with a maximum value of 20 m. Faults are rare (16 in total) and mostly far from the central volcano (Figure 2c). Their main direction ranges from NNE-SSW to NE-SW (81% of data set). The fault throws, mainly normal, are usually of 10–100 cm, with the largest vertical throw of ~40 m. The 75 measured extension fractures are mainly NE-SW trending (64% of data set, Figure 2d), with opening from 0.5 cm to 1 m, focusing between 0.5 and 5 cm. The extension fractures were usually found in proximity of the dikes or the largest fault systems, with limited vertical extent. We anticipate that we could not establish any origin due to tensional (i.e., plate pull) processes.

3.2. The Alftafjordur Central Volcano

In the proximity of the Alftafjordur Central Volcano, the lava pile is often interrupted by ~1 m thick greyish ignimbrites, testifying an explosive activity of the central edifice. Dikes often intrude both the lavas and the greyish ignimbrites. We measured 22 dikes, with scattered strike and mean dip of 63° (Figures 2e and 2f). Their thickness ranges between 0.25 and 3 m, with a mean of 1.7 m and a maximum value of 5 m (Figure 2g). The best outcrops (Kambar shoreline) allow distinguishing two systems of dikes (henceforth called FG and SG) emplaced at different times: an older, NNE-SSW oriented system (FG), represented by thicker (mean of 2.6 m) and steeper dikes (mean dip 80°) and a younger, NNW-SSE oriented system (SG), represented by thinner tangential dikes (mean of 0.7 m) with lower dip (mean 42°), both inward and outward dipping, and thus resembling cone sheets and ring dikes. The extension fractures (40 data) show a main NE-SW direction, whereas no normal faults are observed.

3.3. The Dike Swarm

Along the dike swarm, we measured 165 dikes with main NNE-SSW direction (72% of data set), high dip (between 64° and 90°), and mean thickness of 3.4 m (Figures 2h–2j). To analyze the dike frequency variation along the strike, we merged our observations with previous results [*Gudmundsson*, 1995; *Paquet et al.*, 2007], where the number of dikes across the swarm has been counted in the Alftafjordur, northern Hamarsfjordur, and southern Berufjordur areas. To cover the entire swarm length, we created two additional profiles in southern Hamarsfjordur and northern Berufjordur (Figure 2a). Moreover, where the swarm is partly offshore (sections A and B; Figure S2), we extrapolated the offshore frequency of dikes across the section, in order to cover the entire swarm width. For this, we assumed that along a profile the dike frequency per unit length in the offshore portion is the same as that in onshore portion, so that the number of offshore dikes is proportional to the offshore profile length. Therefore, we used five cross sections with similar length (10 ± 1 km, corresponding to the width of the dike swarm), located at sea level (maximum dike frequency; [*Walker,* 1960]) and progressively farther from the volcanic center (Figure S2). The resulting dike frequency in the profiles along the swarm ranges from 66 (section B, 14 km from the central volcano) to 122 dikes (section D, 22 km from the central volcano).

Across strike, the dike frequency (Figure S3) increases toward the axis of the magmatic system, showing an overall symmetrical pattern. The faults also focus in the areas with the highest dike frequency. The largest fault, with throw of ~40 m, NNE-SSW trending, and 60° dipping, is located in section 4 (see Figure 2a), ~28 km from the volcanic center (Figures S4a, S4c, and S4d). Three dikes are found in the damage zone of the fault, associated with secondary fault planes with normal motion (Figure S4b). The dikes are not faulted and are less fractured that the host rock, suggesting that they intruded at a later stage, after fault nucleation. The 35 extension fractures show a main NNE-SSW direction (54% of the data set) and a more scattered distribution for the rest of the data.

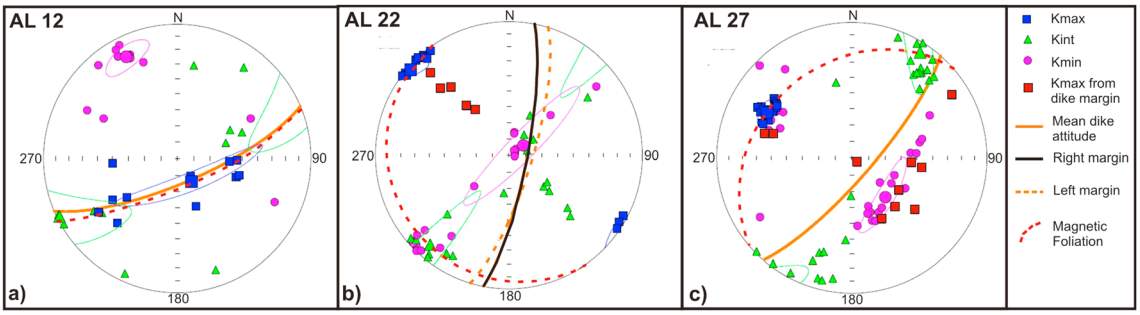

Figure 3. Examples of AMS data from the dike swarm. (a) AMS data from the dike swarm with normal magnetic fabric and subvertical K_{max}. (b) AMS data from the dike swarm, with K_{max} oriented at high angle along the margins and at low angle in the inner part of dikes. (c) AMS data from dike with bimodal flux orientations, parallel to the dike for samples along the margins and orthogonal to the dike in its inner part.

Dike thicknesses and fault horizontal throws along each of the four cross sections were used to calculate the percentage of extension due to diking (Em) and faulting (Et), respectively (Figure 2a), using the following equations:

$$\mathrm{Em} = \frac{S}{L} \times 100 \quad (1)$$

$$\mathrm{Et} = \frac{\mathrm{Rh}}{L} \times 100 \quad (2)$$

where S is the total dike thickness in meters, Rh is the total horizontal fault throw in meters, and L is the length of the section in meters. We obtained Em values of 3%, 1.20%, 1.41%, and 4.02% (±1.30) and Et values of 0.03% and 0.17% (table in Figure 2 for details).

3.4. Kinematic Indicators of Magma Flow Within Dikes

Kinematic indicators, such as slickenlines (due to the flow of magma at the contact with the host rock), elongated vesicles, and minerals, have been recognized on seven dikes sampled for AMS analysis (Table S1). Their orientation is consistent with a subvertical flow for three dikes (AL01, AL24, and AL26) of the dike swarm and a subhorizontal flow for four dikes (AL03, AL04, AL05, and AL06) related to the central volcano.

3.5. Magnetic and Petrofabric Data

The mean susceptibility (K_m) values for the investigated dikes are generally high, ranging from 18×10^{-3} to 107×10^{-3} *SI*, with an average of 59×10^{-3} *SI* (Figure S1). These high values indicate that the magnetic signal is dominantly carried by ferrimagnetic minerals. The AMS ellipsoids have a prolate shape in most of the dikes from the dike swarm, with a gradual variation from oblate to prolate shapes from the margin to the inner part [*Tarling and Hrouda*, 1993]. This shape variation is also accompanied by a variation in the anisotropy degree $(\mathrm{Pj} = \exp\sqrt{2\left[(\ln K_{max} - \eta)^2 + (\ln K_{int} - \eta)^2 + (\ln K_{min} - \eta)^2\right]}$ where $\eta = \frac{\ln K_{max} + \ln K_{int} + \ln K_{min}}{3}$ defined as [*Jelinek*, 1981], Figure S5). The samples from the margin have Pj values common for magmatic rocks (from 1.006 to 1.044), whereas those from the inner part have significantly higher Pj values (from 1.109 to 1.379, Figure S5). In some cases, a typical parabolic shape of the Pj profile is present along sections transverse to the dike plane.

Three dikes have a geometrically normal magnetic fabric with subvertical K_{max} axes (Figure 3a); however, a geometrically inverse magnetic fabric, given by K_{max} axes orthogonal to the dike margins and K_{min} axes subvertical in the dike plane, prevails in 20 dikes. The difference between the geometrically inverse and normal fabric is a switch between K_{max} and K_{min} axes. When both cases are observed within the same dike, the fabric is geometrically normal along preserved dike margin K_{max}, whereas it is geometrically inverse in the inner part of the dike. The K_{int} axes are roughly subhorizontal oriented along the dike plane and often not well clustered (Figure 3). A similar mixture of inverse and normal magnetic fabrics was observed also in dikes from the nearby Reydarfjordur dike swarm [*Kissel et al.*, 2010].

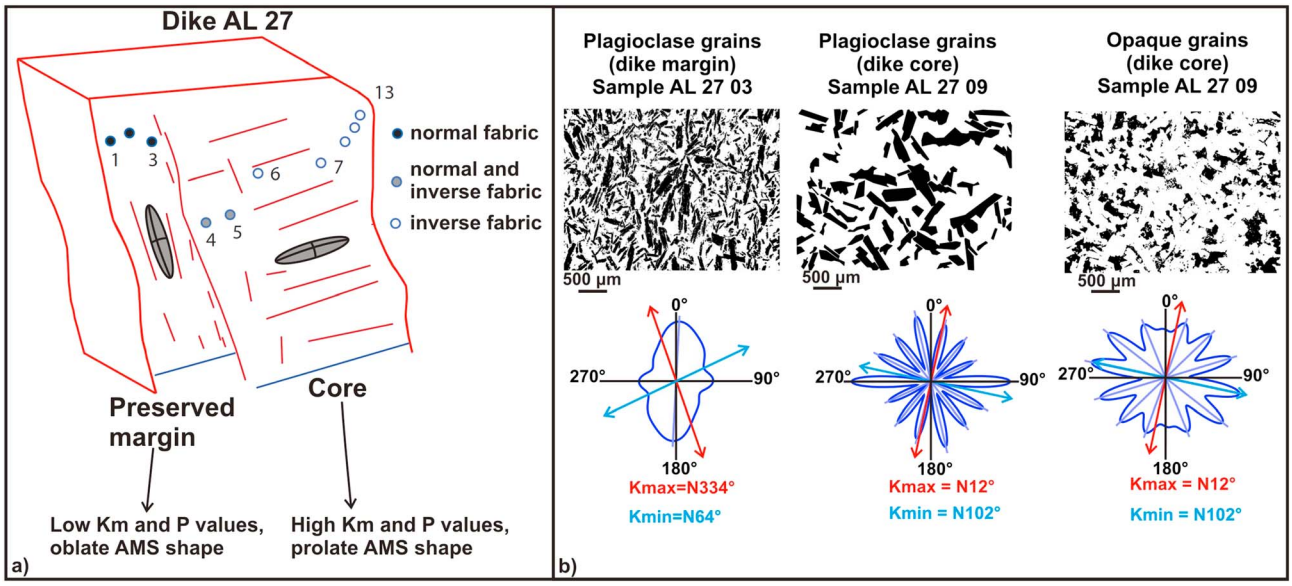

Figure 4. Synthesis of magnetic and petrofabric data along the margin and the inner part of a dike with normal and inverse fabric. (a) Schematic representation of the dike AL27 with sample distribution. (b) Distribution of plagioclase and opaque grains in three thin sections, obtained from the margin to the inner part of the dike AL27. The sections were cut along a plane containing K_{max} and K_{min}. The roses of direction for each phase are sketched below, together with K_{max} and K_{min} orientations. The preserved margin records a primary fabric with a subvertical magma flow direction, whereas the inner part presents an inverse fabric related to secondary processes (see the text for details).

Dikes showing the switch between K_{max} and K_{min} have been further investigated by image analysis from thin sections. Some representative core samples were cut along the plane parallel K_{max} and K_{min} to identify which axis is representative of the preferred orientation of the minerals. While no preferred orientation in phenocrysts or opaque minerals is observed in the inner part of the dike, a petrofabric characterized by preferred orientation of phenocrysts (e.g., plagioclase) is preserved at the dike margins (as dike AL27 in Figure 4). This subvertical preferred orientation of the phenocrysts parallel to the K_{max} axes (Figure 4) indicates that, in the case of geometrically normal magnetic fabric, K_{max} axis is the magmatic flow indicator. In the inner part of most of these dikes, we found a different mineral texture, without preferred orientation of both phenocrysts and opaque minerals (see Figure 4). This behavior is typical of dikes (i.e., AL17, AL22, and AL27) where we observe a progressive migration of K_{max} from vertical to horizontal orientations, from the margin to the inner part. This suggests that, when preserved, the dike margins record the primary magmatic flow with K_{max} axis oriented parallel to the preferred orientation of phenocrysts and opaque minerals, as observed in other cases (e.g., [*Tauxe et al.*, 1998]). This orientation is generally subvertical, consistently with field indicators (Table S1). In the inner part of the dike, there is a reorganization of the phenocrysts and opaque minerals along subhorizontal orientations orthogonal to the dike plane, which does not reflect the original magma emplacement. This fabric could reflect secondary processes producing horizontal readjustment of grains due to lithostatic pressure or during magma cooling stage [*Mattsson et al.*, 2011; *Almqvist et al.*, 2012]. The origin of this geometrically inverse fabric will be discussed elsewhere.

4. Discussion and Conclusions

The dikes proximal to the central volcano, with scattered strike, consist of two generations, with steeper and thicker regional dikes (FG) predating the cone sheets and ring dikes (SG). Conversely, the dikes belonging to the swarm show a consistent NNE-SSW strike. This distribution may result from the stress variations in the different portions of the volcanic system. In the proximal areas, a local stress field favors a tangential distribution of the dikes, which cut preexisting regional dikes, as commonly observed in active volcanoes. In the distal areas, the dike distribution reflects the far field stress (with a WNW-ESE trending σ_3). This bimodal distribution supports existing models on magmatic systems, with ring dikes and cone sheets close to the central volcano and regional dikes along the axis [*Gudmundsson,* 1995, 2006].

The crustal extension due to diking in sections 1 to 4, along the magmatic system, is of 3%, 1.20%, 1.41%, and 4.02% (±1.3), respectively, with a mean value of 2.41%. This is slightly different from what was previously reported, as a mean value of magmatic extension of 5.5% (based on 90 dikes in a single profile) [*Gudmundsson,* 1995], or between 1.036% and 1.046% (sections A and D, respectively, in Figure S2 [*Paquet et al.*, 2007] which face sections 1 and 4 of the present study), or the average magmatic dilation of 5-6% along 4 profiles in NW Iceland [*Gudmundsson*, 1984]. These discrepancies are explained by the different values of L in equation (1): the clustering of the dikes toward the rift center (Figure S3) affects the calculation of the extension when the length of the section includes the system edges.

The extension due to diking, calculated on the four sections far from the central volcano (Figure 2a) is at least 15 times higher than that due to faulting, confirming that at ~1.5 km depth, 95% of crustal extension is accommodated through diking, with negligible role of faulting [*Helgason and Zentilli,* 1985]. The recognized faults are mainly located in areas with the highest dike density. This suggests that either a similar mechanism affects tectonic and magmatic activity along the axis of the magmatic system or that the faults may be dike induced [*Acocella,* 2014, and references therein].

The aspect ratio of the Alftafjordur volcanic system (width/length, measured perpendicular and parallel to the rift axis, respectively) is ~0.29, which, compared against available current spreading rates for divergent plate boundaries (error $<$28%), suggests a much smaller paleo-extension rate, in the order of ~8 mm/yr [*Acocella,* 2014, and references therein]. This value is in agreement with previous estimates based on radiometric data [*Mussett et al.*, 1980] and significantly lower than the present one in the central part of the eastern volcanic zone of Iceland, of ~16 mm/yr [*Perlt et al.*, 2008]. This suggests that crustal spreading in this portion of Iceland may have been significantly slower during the development of the Alftafjordur volcanic system (estimated at 10–12 Ma).

Considering a mean total thickness of the dikes $S \sim 10^2$ m along each section of the magmatic system, as well as a mean spreading rate of ~8 mm/yr, one gets 1.25×10^4 years as the time required to develop the magmatic system. This is roughly consistent with previous estimates, of 10^4 years or slightly less, on the activity of major grabens within magmatic systems, as at Thingvellir (Iceland), Dabbahu (Afar), and Fantale (Main Ethiopian Rift), or 1 order of magnitude smaller than estimates of the entire life span of magmatic systems (0.3 Ma), from inception to extinction, along the Reykjanes Ridge [*Acocella*, 2014, and references therein].

The along-strike dike frequency slightly increases with distance from the central volcano (i.e., from the supposed magma chamber, Figure S2). This implies that at least at this depth, not all the dikes may propagate laterally, as suggested by recent rifting episodes [*Wright et al.*, 2006; *Buck et al.*, 2006; *Sigmundsson et al.*, 2015]. Kinematic field indicators (Table S1) and vertical K_{max} orientation of the dike margins further support a prevalent subvertical propagation of magma in the dike swarm. This fabric has been also recognized in other basaltic dike swarms in Iceland (see *Kissel et al.* [2010]), suggesting that regional dikes are preferentially emplaced in subvertical or inclined flow. Lateral flow may be more common close to the central volcanoes and associated magma chambers, as also suggested by previous studies [*Gautneb and Gudmundsson,* 1992; *Paquet et al.,* 2007; *Eriksson et al.,* 2015]. The inner part of the dikes shows an anomalous (i.e., geometrically inverse) fabric which, in the Reydafjordur region, had been attributed to large Ti-rich magnetite grains formed during the slower cooling process within the dike [*Kissel et al.*, 2010]. Secondary processes at depths of 1–2 km may also be responsible for a partially or totally overprint of the primary fabric, as chemical alterations with different zeolite facies in dikes and lavas of Eastern Iceland, due to postemplacement hydrothermal circulation [*Walker*, 1960]. These fabrics are probably not very informative in terms of magma flow, conversely to those along the dike margins.

Concluding, our study suggests that (1) local variations in the stress field affect dike emplacement in the magmatic system, being the proximal dikes tangential and the distal dikes parallel to the rift axis (NNE-SSW trending); (2) crustal spreading in eastern Iceland at 10–12 Ma was slower than present; (3) the crustal extension, at ~1.5 km of depth, is mainly achieved through diking; and (4) even though recent rifting episodes suggest a lateral magma propagation, a prevalent vertical propagation away from the central volcano, between 1 and 2 km depth, is inferred, consistently with previous results [*Kissel et al.,* 2010]. These results have implications for active crustal spreading along slowly extending divergent plate boundaries, confirming the fundamental role of magmatism (diking), with complex (vertical and horizontal) magma transfer.

Acknowledgments
Joel Ruch and Thor Thordarson provided expert advice and support on the field. Salvatore Pizzichetti provided the thin sections and Massimo Mattei encouraged the use of the Paleomagnetism Laboratory of Roma Tre. A. Gudmundsson and an anonymous reviewer provided helpful suggestions that improved the manuscript. Financed with PRIN 2009 funds (2009H37M59, responsible V. Acocella) and University of Roma Tre MSc thesis project grant (grantee S. Urbani). Any user can access the data of this work by contacting the corresponding author.

The Editor thanks Agust Gudmundsson and an anonymous reviewer for their assistance in evaluating this paper.

References

Acocella, V. (2014), Structural control on magmatism along divergent and convergent plate boundaries: Overview, model, problems, *Earth Sci. Rev.*, *136*, 226–288, doi:10.1016/j.earscirev.2014.05.006.

Almqvist, B. S. G., S. A. Bosshard, A. M. Hirt, H. B. Mattsson, and G. Hetényi (2012), Internal flow structures in columnar jointed basalt from Hrepphólar, Iceland: II. Magnetic anisotropy and rock magnetic properties, *Bull. Volcanol.*, *74*, 1667–1682, doi:10.1007/s00445-012-0622-0.

Blake, D. H. (1969), Welded tuffs and the Maelifell caldera, Alftafjordur volcano, southeastern Iceland, *Geol. Mag.*, *106*, 531–41, doi:10.1017/S0016756800059306.

Blake, D. H. (1970), Geology of the Alftafjordur volcano, a Tertiary volcanic centre in south-east Iceland, *Sci. Icel.*, *2*, 43–63.

Brandsdottir, B., W. Menke, P. Einarsson, R. S. White, and R. K. Staples (1997), Faroe-Iceland Ridge Experiment: 2. Crustal structure of the Krafla central volcano, *J. Geophys. Res.*, *102*, 7867–7886, doi:10.1029/96JB03799.

Buck, W. R., P. Einarsson, and B. Brandsdóttir (2006), Tectonic stress and magma chamber size as controls on dike propagation: Constraints from the 1975–1984 Krafla rifting episode, *J. Geophys. Res.*, *111*, B12404, doi:10.1029/2005JB003879.

Cañón-Tapia, E. (2004), Anisotropy of magnetic susceptibility of lava flows and dykes: A historical account, in *Magnetic Fabric: Methods and Applications*, edited by F. Martin-Hernández et al., *Geol. Soc. London Spec. Publ.*, *238*, 205–225, doi:10.1144/GSL.SP.2004.238.01.14.

Craddock, J. P., B. C. Kennedy, A. L. Cook, M. S. Pawlisch, S. T. Johnston, and M. Jackson (2008), Anisotropy of magnetic susceptibility studies in Tertiary ridge-parallel dykes (Iceland), Tertiary margin-normal Aishihik dykes (Yukon), and Proterozoic Kenora Kabetogama composite dykes (Minnesota and Ontario), *Tectonophysics*, *448*, 115–124, doi:10.1016/j.tecto.2007.11.035.

Desissa, M., N. E. Johnson, K. A. Whaler, S. Hautot, S. Fisseha, and G. J. K. Dawes (2013), A mantle magma reservoir beneath an incipient mid-ocean ridge in Afar, Ethiopia, *Nat. Geosci.*, *6*, 861–865, doi:10.1038/ngeo1925.

Ebinger, C. J., and M. Casey (2001), Continental breakup in magmatic provinces: An Ethiopian example, *Geology*, *29*, 527–530, doi:10.1130/0091-7613(2001)029<0527.

Ebinger, C. J., A. Ayele, D. Keir, J. Rowland, G. Yirgu, T. Wright, M. Belachew, and I. Hamling (2010), Length and timescales of rift faulting and magma intrusion: The Afar rifting cycle from 2005 to present, *Annu. Rev. Earth Planet. Sci.*, *38*(1), 439–466, doi:10.1146/annurev-earth-040809-152333.

Eriksson, P. I., M. S. Riishuus, F. Sigmundsson, and S.-A. Elming (2011), Magma flow directions inferred from field evidence and magnetic fabric studies of the Streitishvarf composite dike in east Iceland, *J. Volcanol. Geotherm. Res.*, *206*, 30–45, doi:10.1016/j.jvolgeores.2011.05.009.

Eriksson, P. I., M. S. Riishuus, and S.-A. Elming (2015), Magma flow and palaeo-stress deduced from magnetic fabric analysis of the Álftafjörður dyke swarm: Implications for shallow crustal magma transport in Icelandic volcanic systems, in *The Use of Palaeomagnetism and Rock Magnetism to Understand Volcanic Processes*, edited by H. M. Ort, M. Porreca, and J. W. Geissman, *Geol. Soc. London Spec. Publ.*, *396*, 107–132, doi:10.1144/SP396.6.

Gautneb, H., and A. Gudmundsson (1992), Effect of local and regional stress-fields on sheet emplacement in West Iceland, *J. Volcanol. Geotherm. Res.*, *51*, 339–356, doi:10.1016/0377-0273(92)90107-O.

Gudmundsson, A. (1983), Form and dimensions of dykes in eastern Iceland, *Tectonophysics*, *95*, 295–307, doi:10.1016/0040-1951(83)90074-4.

Gudmundsson, A. (1984), Tectonic aspect of dykes in northwestern Iceland, *Jokull*, *34*, 81–96.

Gudmundsson, A. (1995), Infrastructure and mechanics of volcanic systems in Iceland, *J. Volcanol. Geotherm. Res.*, *64*, 1–22, doi:10.1016/0377-0273(95)92782-Q.

Gudmundsson, A. (2006), How local stresses control magma-chamber ruptures, dyke injections, and eruptions in composite volcanoes, *Earth Sci. Rev.*, *79*, 1–31, doi:10.1016/j.earscirev.2006.06.006.

Gudmundsson, A., N. Lecoeur, N. Mohajeri, and T. Thordarson (2014), Dike emplacement at Bardarbunga, Iceland, induces unusual stress changes, caldera deformation, and earthquakes, *Bull. Volcanol.*, *76*, 1–7, doi:10.1007/s00445-014-0869-8.

Helgason, J., and M. Zentilli (1985), Field characteristics of laterally emplaced dikes: Anatomy of an exhumed Miocene dike swarm in Reydarfjordur, eastern Iceland, *Tectonophysics*, *115*, 247–274, doi:10.1016/0040-1951(85)90141-6.

Jelinek, V. (1981), Characterization of the magnetic fabric of rocks, *Tectonophysics*, *79*, 63–67, doi:10.1016/0040-1951(81)90110-4.

Kissel, C., C. Laj, H. Sigurdsson, and H. Guillou (2010), Emplacement of magma in Eastern Iceland dikes: Insights from magnetic fabric and rock magnetic analyses, *J. Volcanol. Geotherm. Res.*, *191*, 79–92, doi:10.1016/j.jvolgeores.2009.12.008.

Launeau, P., C. J. Archanjo, D. Picard, L. Arbaret, and P.-Y. Robin (2010), Two- and three-dimensional shape fabric analysis by the intercept method in grey levels, *Tectonophysics*, *492*(1–4), 230–239, doi:10.1016/j.tecto.2010.06.005.

Mattsson, H. B., L. Caricchi, B. S. G. Almqvist, M. J. Caddick, S. A. Bosshard, G. Hetényi, and A. M. Hirt (2011), Melt migration in basalt columns driven by crystallization-induced pressure gradients, *Nat. Commun.*, *2*(299), 1–6, doi:10.1038/ncomms1298.

Moorbath, S., H. Sigurdsson, and R. Goodwin (1968), K-Ar ages of oldest exposed rocks in Iceland, *Earth Planet. Sci. Lett.*, *4*, 197–205, doi:10.1016/0012-821X(68)90035-6.

Mussett, A. E., J. G. Ross, and I. L. Gibson (1980), $^{40}Ar/^{39}Ar$ dates of eastern Iceland lavas, *Geophys. J. R. Astron. Soc.*, *60*, 37–52.

Paquet, F., O. Dauteuil, E. Hallot, and F. Moreau (2007), Tectonics and magma dynamics coupling in a dyke swarm of Iceland, *J. Struct. Geol.*, *29*, 1477–1493, doi:10.1016/j.jsg.2007.06.001.

Perlt, J., M. Heinert, and W. Niemeier (2008), The continental margin in Iceland—A snapshot derived from combined GPS networks, *Tectonophysics*, *447*, 155–166, doi:10.1016/j.tecto.2006.09.020.

Rochette, P., C. Aubourg, and M. Perrin (1999), Is this fabric normal? A review and case studies in volcanic formations, *Tectonophysics*, *307*, 219–234, doi:10.1016/S0040-1951(99)00127-4.

Sigmundsson, F., et al. (2015), Segmented lateral dyke growth in a rifting event at Bárðarbunga volcanic system, Iceland, *Nature*, *517*, 191–195, doi:10.1038/nature14111.

Tarling, D. H., and F. Hrouda (Eds.) (1993), *The Magnetic Anisotropy of Rocks*, 217 pp., Chapman and Hall, London.

Tauxe, L., J. S. Gee, and H. Staudigel (1998), Flow directions in dikes from anisotropy of magnetic susceptibility data: The bootstrap way, *J. Geophys. Res.*, *103*, 17,775–17,790, doi:10.1029/98JB01077.

Walker, G. P. L. (1958), Geology of the Reydarfjordur area, eastern Iceland, *Q. J. Geol. Soc. London*, *114*, 367–391, doi:10.1144/gsjgs.114.1.0367.

Walker, G. P. L. (1960), Zeolite zones and dyke distribution in relation to the structure of the basalts of eastern Iceland, *J. Geol.*, *68*, 515–528.

Walker, G. P. L. (1963), The Breiddalur central volcano, eastern Iceland, *Q. J. Geol. Soc. London*, *119*, 29–63, doi:10.1144/gsjgs.119.1.0029.

Walker, G. P. L. (1974), The structure of eastern Iceland, in *Geodynamics of Iceland and the North Atlantic Area, Proceedings of the NATO Advanced Study Institute Held in Reykjavík, Iceland, 1–7 July 1974*, edited by L. Kristjansson, pp. 177–188, D. Reidel, Dordrecht, Netherlands, doi:10.1007/978-94-010-2271-2_12.

Wright, T. J., C. Ebinger, J. Biggs, A. Ayele, G. Yirgu, D. Keir, and A. Stork (2006), Magma maintained rift segmentation at continental rupture in the 2005 Afar dyking episode, *Nature*, *442*, 291–294, doi:10.1038/nature04978.